JOURNAL OF APPLIED ELECTROCHEMISTRY 25 (1995) 962–966

The fractal dimension of corroded aluminium surfaces

P. R. ROBERGE

Royal Military College, Kingston, Ontario, K7K 5LO, Canada

K. R. TRETHEWEY

University of Southampton, Southampton, SO17 1BJ, Great Britain

Received 26 September 1994; revised 30 January 1995

The nature of surface features produced during the corrosion of a metallic surface is an important parameter that can affect both the corrosion kinetics and the response of the interface to electrochemical probing. These features are so visibly present, when the surface properties are studied over a certain frequency range, that scientists have recognized and attempted to model them for almost seventy years. But while the evidence is high that many of these features are probably related to the fractal nature of the surface, actual experimental evidence is still quite scarce. In this paper an attempt is made to correlate the fractal dimension of surface profiles measured with a commercial instrument on corroded aluminium specimens with results obtained with electrochemical impedance spectroscopy (EIS).

1. Introduction

Surface modifications occurring during the degradation of a metallic material can greatly influence the subsequent behaviour of the material. These modifications can also affect the electrochemical response of the material if it is submitted to a voltage or a current perturbation. Fortunately, models based on fractal and chaos mathematics have been developed to describe complex shapes and structures and explain many phenomena encountered in science and engineering [1–3]. These models have been applied to different fields of materials engineering, including corrosion studies. Fractal models have, for example, been used to explain the frequency dependency of a surface response to probing by electrochemical impedance spectroscopy (EIS) [4–11] and more recently to explain some of the features observed in the electrochemical noise generated by corroding surfaces [12, 13]. Fractal mathematics have also been used to explain the pit morphology of a corrosion situation [14]. Unfortunately, experiments are much scarcer than theories. In a recent paper discussing the theories explaining the origin of dispersion effects observable by EIS, only one paper was said to have attempted to correlate the roughness of metallic surfaces with fractal theories [15]. The authors of this paper reported having not found any correlation between the constant phase angle (CPA) obtained from EIS measurements and the fractal dimension obtained by analysing surface profiles of blocked electrodes exposed to 0.1 M H_2SO_4 solution [16]. In the present paper, fractal and stochastic mathematics have been applied to surface profiles measured with a commercial instrument and the results obtained were compared to the fractal dimension speculated from EIS measurements made under similar conditions.

2. Experimental details

2.1. *Surface profile experiments*

A sample of rolled aluminium 2024 sheet (nominal composition 0.5% Si, 0.5% Fe, 4.3% Cu, 0.6% Mn, 1.5% Mg, 0.25% Zn) of dimensions 100 mm × 40 mm × 4 mm and polished to a 600 grit finish, was placed in a 250 ml beaker such that it was immersed in aerated 3% NaCl solution to a level about 30 mm from the top of the specimen. All experiments were conducted at ambient temperature (~ 20 °C). The effect of aeration created a 'splash zone' over the surface of the specimen which was not immersed. During the course of exposure, a portion of the immersed region in the centre of the upward-facing surface became covered in gas bubbles and suffered a higher level of attack than the rest of the immersed surface. After 24 h the plate was removed from the solution. Figure 1 shows in diagrammatic form the specimen and areas from which the surface profiles were measured.

Surface profile measurements were made by means of a Rank Taylor Hobson Form Talysurf with a 0.2 μm diamond tip probe in all of the various planes, (i.e., LT, TL, LS, SL, ST and TS). The instrument created a line scan of a real surface by pulling the probe across a predefined part of the surface at a fixed scan rate of 1 mm s^{-1}. All traces were of length 8 mm, generating 32 000 points with a sampling rate of 0.25 μm per point, except for the SL and ST directions which, because of the plate thickness, were limited to 2 mm traces or 8000 points. The manufacturer's software for the Talysurf instrument was capable of generating over twenty surface profile parameters. In this study two parameters, *Ra* and *Rt* were retained. *Ra*, the

0021-891X/93

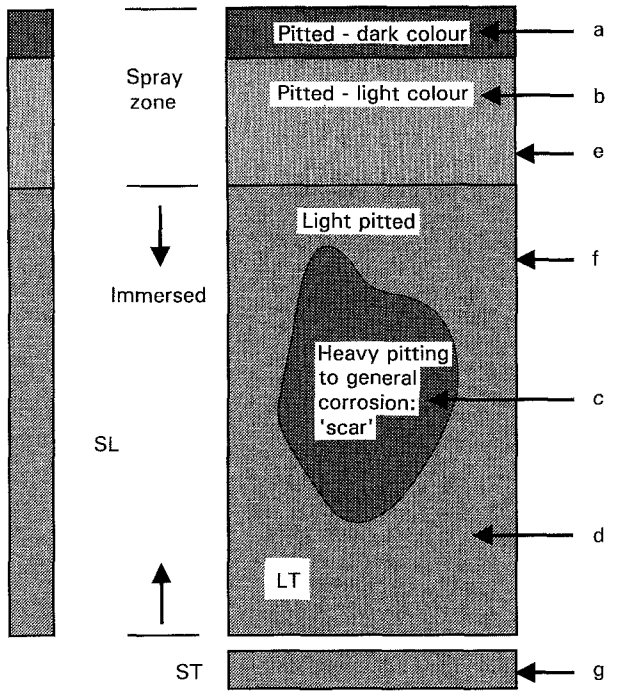

Fig. 1. Diagram of aluminium sheet specimen with locations of corroded zones.

roughness average, described the average deviation from a mean line, while *Rt* described the distance from the deepest pit to the highest peak of the profile, an index which was taken as an engineering 'worst case' parameter for pitting severity.

2.2. *Electrochemical impedance spectroscopy experiments*

The aluminium specimens tested in the present study were cut from commercial sheet material (thickness 1.0 mm) to appropriate sizes for mounting in epoxy according to metallographic techniques. The samples were mounted in a manner that would expose only one face of each of three orthogonal planes related to the rolling direction of the sheet. Prior to mounting, provisions were made for electrical connection to the unexposed back of the samples and the unexposed edges were coated with an aluminium-vinyl anti-corrosive paint to prevent crevice corrosion between the epoxy mount and the aluminium electrodes. After mounting, the specimens were polished (using 240, 400 and finally 600 grit papers) and washed with water followed by acetone and dichloromethane.

For each experiment, a pair of identical aluminium specimens (same exposed face) were immersed in a 2 dm^3 beaker containing a solution of 3% sodium chloride. Each cell was equipped with an air purge and a saturated calomel electrode (SCE) brought into close proximity to one aluminium specimen by a Luggin probe. The mounted specimens were separated by 2.5 mm and kept in a stable parallel position with plastic holders. The electrochemical impedance spectroscopy (EIS) measurements were performed with a commercial generator/analyser (Solartron model 1255) at the corrosion potential. The starting frequency (100 Hz), the number of frequencies (25) and the frequency intervals ($\log \Delta f = -0.125$) were similar for all measurements. The alternating current was applied directly between the two aluminium electrodes and kept at a value which did not cause more than 10 mV difference (peak to peak) across the cell. The corrosion potentials were recorded at regular intervals by measuring the potential difference between the SCE and the exposed aluminium specimens.

3. Results and discussion

3.1. *Surface profiles experiments*

The corrosion found on the plate varied considerably from area to area. The region of the plate beneath the gas bubbles was found to be particularly corroded, the concentration of pits being very high. Across the remainder of the immersed upward-facing surface, the pitting was scattered. The 'splash zone' of the surface above the electrolyte was also badly pitted. On the sides, pits had a geometry and orientation which conformed to the expected grain structure of the rolled material. In all cases, the changes noted in traditional Talysurf parameters were consistent with expectations. Severity of corrosion was indicated by increase in *Ra* and *Rt* and the profiles obtained gave good general indications of the degree of pitting and the size of pits. There was an approximate tenfold increase in *Ra* and *Rt* between the freshly polished surface (the 'Ref' in Table 1)and the heavily corroded profiles such as a, b, e and g.

All the profiles measured and analysed with the Talysurf equipment were also analysed with the rescaled range (R/S) analysis technique. The R/S technique, which can provide a direct evaluation of the fractal dimension of a signal, was derived from one of the most useful mathematical models for analysing time-series data proposed a few years ago by Mandelbrot and van Ness [17]. A detailed description of the R/S technique (where R or $R(t,s)$ stands for the sequential range of the data points increments for a given lag s and time t, and S or $S(t,s)$ for the square root of the sample sequential variance) can be found in Fan *et al.* [18]. Hurst [19] and later Mandelbrot and Wallis [20] have proposed that the ratio $R(t,s)/S(t,s)$, also called the rescaled range, was itself

Table 1. Calculated surface parameters for regions identified on Fig. 1

Plane	*Zone*	*Ra* /μm	*Rt* /μm	*D*
	Ref*	0.14	2.95	1.45
LT	a	1.12	17.6	1.27
	b	1.36	20.0	1.27
	c	0.48	8.82	1.36
	d	0.71	12.8	1.42
SL	e	1.59	15.7	1.23
	f	0.84	14.9	1.30
ST	g	1.01	17.6	1.35

* Average reference trace measured before corrosion exposure.

a random function with a scaling property described by Relation 1 where the scaling behaviour of a signal is characterized by the Hurst exponent (H), also called scaling parameter, which can vary between $0 < H < 1$.

$$\frac{R_{(t,s)}}{S_{(t,s)}} \propto s^H \tag{1}$$

It has additionally been shown [21] that the local fractal dimension D of a signal is related to H through Equation 2 which makes it possible to characterize the fractal dimension of given time series by calculating the slope of a R/S plot.

$$D = 2 - H \quad \text{for} \quad 0 < H < 1 \tag{2}$$

Examining the data in Table 1 it is apparent that the ground, uncorroded surfaces both exhibited behaviour close to that of a Brownian profile for which the fractal dimension D equals 1.5 [20, 21]. The corroded areas with the largest reduction in D were those with the most pitting, that is, traces a, b and e, all of which occurred in the spray zone above the water. The reduction in fractal dimension at the fine texture resolution of the Talysurf, from about 1.5 to about 1.2, would indicate a 'smoothing' which might be explained from a greater loss of mass from the peaks than from the valleys of the profiles. The correlation coefficients between the fractal dimension and the surface parameters presented in Table 1 were calculated to be 0.89 for *Ra* and 0.76 for *Rt*. This would indicate that the fractal dimension is slightly better related to a short range descriptor or an average quantity such as *Ra* than to a longer range descriptor or a worst case distance quantity such as *Rt*.

3.2. *EIS experiments*

The EIS measurements were analyzed with the projection–permutation (ProPer) method that has been used successfully both for field corrosion monitoring and routine laboratory work [23, 24]. A previous study of the corrosion behaviour of various aluminium sheet materials, exposed to an aerated saline solution, had revealed that the depression angle from the real axis in a complex plane representation of EIS results, which is almost an omnipresent character of EIS measurements, was related to the susceptibility of each alloy to localized corrosion [25]. In fact, this study demonstrated that the depression angle was a more reliable indicator of localized corrosion than the polarization resistance (R_p) values proved to be of the general corrosion rates.

The presence of such depression is not a new observation. In reality, the scaling property of complex impedance ($Z(\omega)$) of real electrodes was reported as early as 1926 [26]. This phenomenon seemed to obey what became known as the CPA scaling relation (Equation 3) that expresses $Z(\omega)$ as a function of frequency (ω), current (i) and a CPA (β) [27].

$$Z(\omega) \propto (i\omega)^{-\beta} \tag{3}$$

The CPA has often been introduced in mathematical fitting of EIS data as an empirical factor which would appear as an exponent added to the imaginary term of

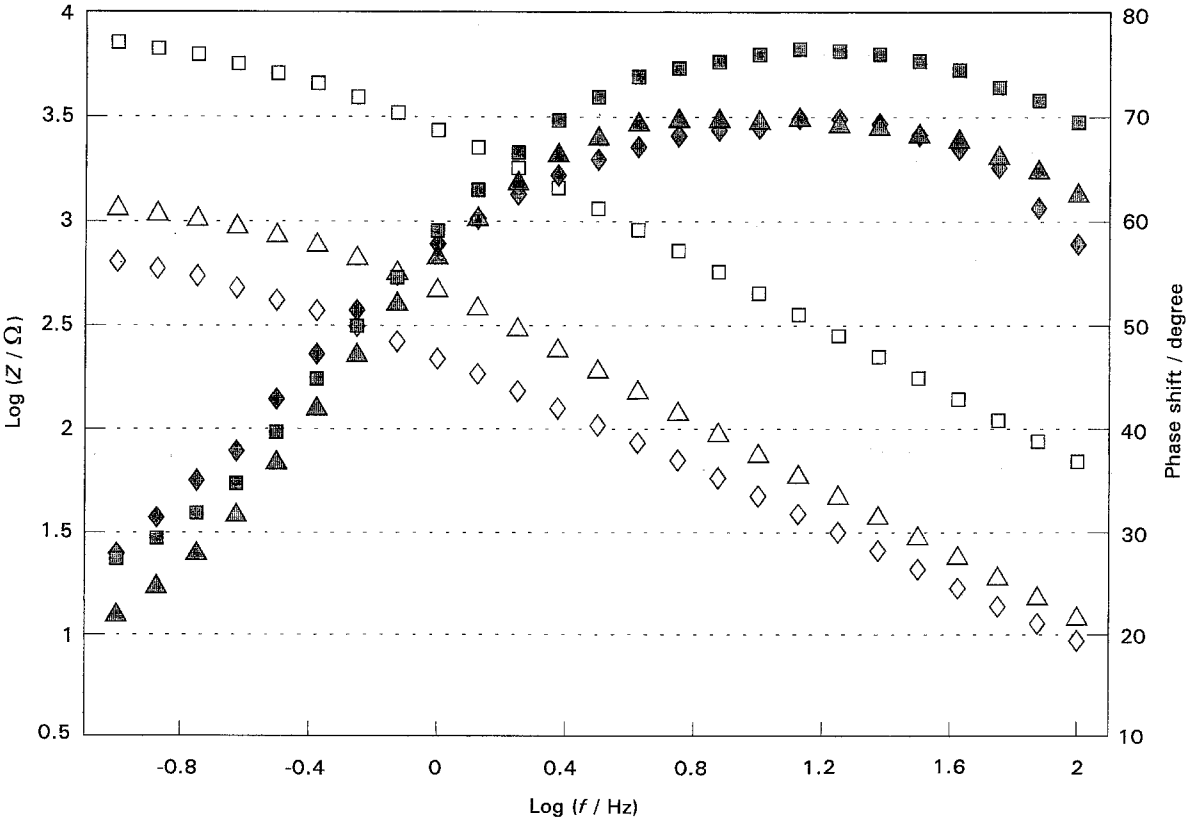

Fig. 2. EIS Bode plots of impedance (white) and phase shift (grey) of 2024-T3 sheet material from EIS results obtained after 24 h exposure to an aerated 3% NaCl solution: (□) LT, (△) SL, (◇) ST.

Table 2. Average CPA measured with EIS for 2024-T3 sheet specimens exposed to a 3% aerated NaCl solution during 24 h

Plane	*Dep*	β	$3-\beta$*	$1+1/\beta^{\dagger}$	$(5-\beta)/2^{\ddagger}$	$1+2\beta^{\S}$
Ref	11.0[‖]	0.88	2.12	2.14	2.06	2.76
LT	17.9	0.80	2.20	2.25	2.10	2.60
	17.3	0.81	2.19	2.24	2.10	2.62
SL	23.1	0.74	2.26	2.35	2.13	2.49
	17.0	0.81	2.19	2.23	2.09	2.62
ST	28.0	0.69	2.31	2.45	2.16	2.38
	26.8	0.70	2.30	2.42	2.15	2.40

Proposed relations between the CPA (β) and the fractal dimension of the interface according to [7, 8]*, [10]†, [35]‡ and [36]§.
[‖] Average depression angle measured with any metallic surface polished to 600 grit [37].

an RC circuit model [28, 29]. Figure 2 illustrates some typical results obtained with the 2024-T3 aluminium specimens exposed to an aerated 3% sodium chloride solution. One can easily obtain the CPA from the straight portion, typically between 1 Hz and 100 Hz in Fig. 2, of the impedance Bode plots. In this particular example the CPA would be 0.80 for the LT specimen, 0.78 for SL and 0.70 for ST.

It has been demonstrated experimentally that the CPA element originates from the microscopic roughness of the interface [30–32]. During a study of carbon steel resistance to corrosion, a practical correlation was even established between pit depth measurements and the cumulative depression angle calculated from EIS data [33]. Some noteworthy predictions [27] have been used to convert the CPA, obtained during the experiments with EIS, into the fractal dimension of the studied surfaces (Table 2). These results were then compared to the surface profilometry results presented in Table 1 since the scaling parameter is dimension invariant [34], that is, for the EIS results presented in Table 2 one would expect D to vary between 2 and 3 since the EIS results describe a surface response to a probing frequency while the results in Table 1 describe only a section of the surface with D between 1 and 2.

It is obvious that none of the scaling parameters predicted with the models in Table 2 fitted completely the results obtained by surface profilometry. But only one model [36] attributed a higher value to the fractal dimension of the reference material, a phenomenon repetitively observed during the analysis of the surface profile measurements. The other three models considered clearly indicated that an uncorroded surface had lower fractality than corroded surfaces. A possible explanation for this discrepancy and the general lack of fit could be that the formalisms employed to relate β to D in these models do not take into account faradaic processes and only describe ideally polarized surfaces. A more realistic approach would be to use more complex relations to describe the multifractal nature of such surfaces [27].

4. Conclusion

R/S analysis can provide a direct method for determining the fractal dimension of surface profiles measured with commercial equipment. Simple correlations were established between conventional surface profile calculations and the fractal dimension revealed by the R/S analysis. Such analysis was helpful in shedding a new light on the real nature of the microscopic transformations occurring during the corrosion of aluminium. A comparison between the surface profile results and the fractal dimensions estimated with published models relating the CPA, an omnipresent characteristic of EIS results, to the fractal dimension indicated that none of these models explained fully the behaviour observed by surface profilometry. Some work is still required to develop new models of corroding interfaces that would take into account the electrochemical processes that are bound to affect the measurements by EIS, for example.

References

[1] E. Lorenz, *J. Atmosph. Sci.* **20** (1963) 448.
[2] M. Feigenbaum, *J. Statist. Phys.* **19** (1978) 25.
[3] B. B. Mandelbrot, The fractal geometry of nature, W. H. Freeman & Co., New York, (1983).
[4] R. de Levie, *J. Electroanal. Chem.* **281** (1990) 1.
[5] A. Le Mehaute, G. Marcellin and G. Crepy, *Compt. Rend.* **303** (1982) 769.
[6] S. H. Liu, *Phys. Rev. Lett.* **55** (1985) 529.
[7] T. Kaplan, S. H. Liu and L. J. Gray, *Phys. Rev. B* **35** (1987) 5379.
[8] B. Sapoval, J.-N. Chazalviel and J. Peyriere, *Phys. Rev. A* **38** (1988) 5867.
[9] J. C. Wang, *Electrochim. Acta* **33** (1988) 707.
[10] T. Pajkossy and L. Nyikos, *J. Electrochem. Soc.* **133** (1986) 2063.
[11] M. Keddam and H. Takenouti, *Compt. Rend.* **302** (1986) 281.
[12] P. R. Roberge, *J. Appl. Electrochem.* **23** (1993) 1223.
[13] A. Legat and E. Govekar, *Fractals* **2** (1994) 241.
[14] R. Reigada, F. Sagues and J. M. Costa, 'Computer Simulation of Pitting Corrosion', *in* 'Progress in the understanding and prevention of corrosion', (edited by J. M. Costa and A. D. Mercer), The Institute of Materials, London (1993).
[15] T. Pajkossy, *J. Electroanal. Chem.* **364** (1994) 111.
[16] J. B. Bates, Y. T. Chu and W. T. Stribling, *Phys. Rev. Lett.* **60** (1988) 627.
[17] M. W. Joosten, T. Johnsen, H. H. Hardy, T. Jossang and J. Feder, 'Fractal Behaviour of CO_2 Pits', CORROSION 92, paper 11, National Association of Corrosion Engineers, TX (1992).
[18] B. B. Mandelbrot and J. W. Van Ness, *SIAM Rev.* **10** (1968) 421.
[19] L. T. Fan, D. Neogi and M. Yashima, 'Elementary introduction to spatial and temporal fractals', Springer-Verlag, Berlin (1991).
[20] E. H. Hurst, *Proc. Inst. Civil Engng* **5** Part I (1956) 519.
[21] B. B. Mandelbrot and J. R. Wallis, *Water Res. Res.* **5** (1969) 321.
[22] J. Feder, 'Fractals', Plenum, New York (1988).
[23] P. R. Roberge and V. S. Sastri, *Corrosion* **50** (1994) 744.
[24] P. R. Roberge, 'A Critical Description of the Permutation of EIS Data Points Technique for Corrosion Measurements and Monitoring', Proceedings of CORROSION 94, National Association of Corrosion Engineers, Houston (1994), paper 318.
[25] P. R. Roberge, E. Halliop, D. R. Lenard and J. Moores, *Corros. Sci.* **35** (1993) 213.
[26] I. Wolff, *Phys. Rev.* **27** (1926) 755.
[27] A. E. Larsen, D. G. Grier and T. C. Halsey, *Fractals* **2** (1994) 191.
[28] D. C. Silverman and J. E. Carrico, *Corrosion* **45** (1988) 280.
[29] I. Epelboin and M. Keddam, *J. Electrochem. Soc.* **117** (1970) 1082.
[30] R. de Levie, *Electrochim. Acta* **10** (1965) 113.

[31] P. H. Bottelberghs and G. H. J. Broers, *J. Electroanal. Chem.* **72** (1976) 257.
[32] J. B. Bates, J. C. Wang and Y. T. Chu, *Solid State Ionics* **18** and **19** (1986) 1045.
[33] P. R. Roberge, V. S. Sastri and E. Halliop, *Corrosion* **48** (1992) 333.
[34] R. F. Voss, 'Fractals in Nature: From Characterization to Simulation', *in* 'The science of fractal images', (edited by H. O. Peitgen and D. Saupe), Springer-Verlag, New York (1988) p. 21.
[35] T. R. Halsey, *Phys. Rev. A* **35** (1987) 3512.
[36] L. Nyikos and T. Pajkossy, *Electrochim. Acta* **31** (1986) 1347.
[37] U. Rammelt and G. Reinhard, *ibid.* **35** (1986) 1045.